PCCP

Shock wave study of the unimolecular dissociation of H_2O_2 in its falloff range and of its secondary reactions

Ch. Kappel, K. Luther and J. Troe*

Institut für Physikalische Chemie, Universität Göttingen, Tammannstraße 6, D-37077, Göttingen, Germany

Received 7th May 2002, Accepted 10th July 2002
First published as an Advance Article on the web 9th August 2002

The thermal decomposition of H_2O_2 was studied behind reflected shock waves using absorption spectroscopy at 215 nm with light from a laser source and at 215, 230, and 290 nm with light from a UV lamp. Due to the improved detection sensitivity for H_2O_2 and HO_2, rate constants for the reactions H_2O_2 (+Ar) $\rightarrow$ 2HO (+Ar) (1), $HO_2 + HO_2 \rightarrow H_2O_2 + O_2$ (3) and $HO + HO_2 \rightarrow H_2O + O_2$ (4) could be derived with much better precision than possible in earlier work. Rate constant minima for reactions (3) and (4) near 800 and 1100 K, respectively, were reconfirmed. Falloff curves of reaction (1) near to the low pressure limit were measured in experiments at about 1, 4, and 15 bar. Limiting low pressure rate constants for reaction (1) of about $k_{1,0} = [Ar]10^{16.36\pm0.23}\exp[-21\,962(\pm608)\ K/T]\ cm^3\ mol^{-1}\ s^{-1}$ were obtained over the temperature range 950–1250 K. The deviations from the low pressure limit at relatively low pressures may provide experimental evidence for non-exponential lifetime distributions of dissociative H_2O_2 such as recently observed in classical trajectory calculations on the *ab initio* potential of H_2O_2.

1. Introduction

Shock wave studies of the pyrolysis of hydrogen peroxide[1–7] offer a number of opportunities. First, the dissociation reaction

$$H_2O_2(+M) \rightarrow 2HO\ (+M) \qquad (1)$$

can be studied under high temperature conditions, complementing measurements at lower temperatures from static and flow systems.[8–13] At the same time, dissociation results can be compared with measurements[14–17] of the reverse recombination reaction

$$2HO(+M) \rightarrow H_2O_2\ (+M) \qquad (-1)$$

.

Since low temperature studies of reaction (−1) covered the full range from low pressure third order to high pressure second order recombination, it is of interest whether the corresponding transition from low pressure second order to high pressure first order dissociation can also be observed under high temperature pyrolysis conditions.

Second, reaction (1) provides an access to a series of secondary reactions which are of importance in the field of combustion. These are the reactions

$$HO + H_2O_2 \rightarrow HO_2 + H_2O \qquad (2)$$

$$HO_2 + HO_2 \rightarrow H_2O_2 + O_2 \qquad (3)$$

$$HO + HO_2 \rightarrow H_2O + O_2. \qquad (4)$$

In shock wave experiments, these processes are observable most directly through UV absorption signals of HO_2[2,5] and HO.[7] All of these reactions are characterized by unusual highly non-Arrhenius temperature dependences.[18]

Finally, the considered experiments also allow the measurement of the UV absorption spectra of H_2O_2 and of HO_2 under high temperature conditions. The UV spectrum of HO_2 in the gas phase was detected in shock wave studies of the pyrolysis of H_2O_2.[2] In combination with later measurements at lower temperatures,[19,20] the temperature dependence of the absorption coefficient could be established over a wide range which allows for conclusions on the shape of the excited state potential.[4] Similar investigations for the spectrum of H_2O_2 were made.[4]

Since potential energy surfaces of reaction systems like (1)–(4) are becoming accessible now from accurate *ab initio* determinations (see *e.g.*[21,22] for H_2O_2) and rate calculations on these potentials can be made, it appears desirable to have the most reliable experimental results for the rate constants of reactions (1)–(4). In looking at the available data, two problems are obvious: high temperature results come only from one laboratory (our own) and a number of experimental problems may not have been overcome in earlier work to the desired extent. The first problem calls for independent measurements in other laboratories. The second problem motivated us to visit the system again, with much improved experimental and numerical possibilities. In particular, we were interested to reliably establish the small deviations from second order in reaction (1) which appeared to be just observable in earlier shock wave studies.[1] In addition, we were keen to confirm the observation of rate constant minima of reactions (3) and (4) suggested by our earlier work and to establish the widths of the rate constant minima. We hope that an independent confirmation of these results from other laboratories will become available in the future.

2. Experimental technique

Our experiments were done in an aluminium shock tube of 10 cm inner diameter, having a low pressure section of 4.15 m and a high pressure driver section of 2.80 m length. The driver gas was H_2, and the reaction mixtures consisted of Ar and traces of H_2O_2. Dissociation experiments were performed in reflected shock waves and monitored through quartz windows mounted 4.5 cm before the reflecting end plate. Shock

 DOI: 10.1039/b204364e

wave conditions were calculated from the velocity of the incident shock wave, determined with the signals from 4 platinum resistance stations over the last 1.30 m before the end plate. Simultaneously, pressure–time profiles were recorded. Since our technique was standard and our experimental set up has been described before,[5] only few details are described in the following.

The mechanism of reactions (1)–(4) is influenced by the initial concentration $[H_2O_2]_0$ of the parent molecule behind the reflected shock. For this reason, considerable attention was paid to the *in situ* determination of this quantity. H_2O_2 (70% from Solvay Interox) was repeatedly vapourized in a saturator and the water content during this procedure was monitored *via* the vapour pressure. At the end of the procedure practically pure (>99%) H_2O_2 was produced, stored at 0 °C, and introduced into the shock tube with a flow of the carrier gas Ar through the saturator and an inlet valve in the end plate. The concentration of the reaction mixture before the shots was determined by in situ detection of H_2O_2 through its light absorption at 215 nm. For this measurement, the frequency-quadrupled light of a mode locked Ti:sapphire laser (Spectra Physics Tsunami pumped by a Nd:YVO_4 laser Millennia X, 80 fs pulses at 82 MHz reprate) traversed the shock tube up to 11 times through planar windows perpendicular to the observation windows. The use of planar windows created some perturbations of the shock waves; these were shown, however, to be negligible for temperatures behind the reflected waves below 1400 K. The precision of the shock wave conditions of our present set up was controlled by test experiments with N_2O/Ar mixtures, monitoring the particularly well known thermal dissociation of N_2O. Since the accurate determination and monitoring of the H_2O_2 concentration was of great importance, continuous observation of H_2O_2 concentrations during the filling procedure of the tube was necessary. In order to avoid wall decomposition of H_2O_2, the reaction mixture came into contact only with aluminium, glass, and Teflon. Reaction mixtures of 0.1–0.3 percent of H_2O_2 in Ar generally were employed. In our earlier experiments, it was assumed that some residual concentrations of H_2O and the wall decomposition product O_2 necessitated a correction of the shock temperatures of about 2–3 percent.[4] The present experiments by continuous monitoring of the H_2O_2 concentrations, during the filling procedure of the shock tube, after closing of the tube, and during varying time delays before starting the run, clearly showed that this correction was not required, see below.

The pyrolysis reaction was followed by recording absorption-time signals of H_2O_2 and HO_2 over the wavelength range of 215–290 nm. Light sources of our absorption measurements behind the shock waves were either the laser described above with single or threefold traversal of the tube, or a standard high pressure Xe lamp. Optimum signals were obtained with threefold tube traversal of the analysis light from the laser. The quality of the absorption signals by far exceeded that of our first experiments[1,2] while the general features of the signals remained unchanged. Fig. 1 compares signals at 215 nm obtained with threefold tube traversal of laser light or with single tube traversal of lamp light. Fig. 2 shows a series of signals recorded at 215 nm for different temperatures. In all these examples, the superposition of the absorptions of the disappearing H_2O_2 and of the forming and finally also disappearing HO_2 is clearly documented.

3. Experimental results

3.1 Absorption coefficients of H_2O_2

Since the *in situ* concentration of H_2O_2 in the reaction mixtures was determined through the room temperature absorption at

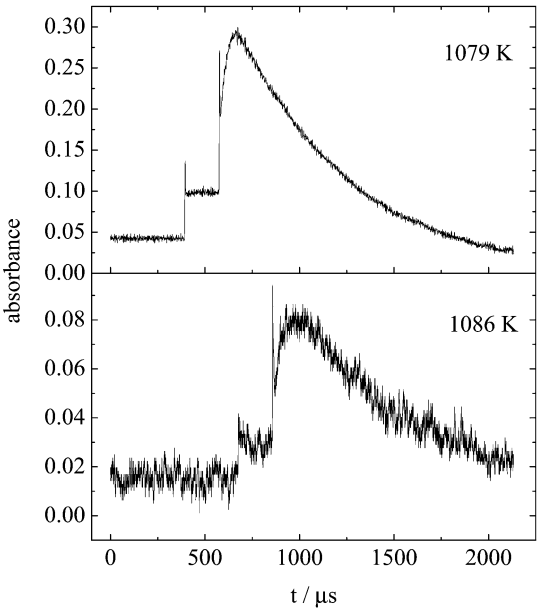

Fig. 1 Absorption signals at 215 nm (upper panel: threefold tube traversal of laser light, $T = 1079$ K, $[H_2O_2]_0/[Ar] = 1.954 \times 10^{-3}$, $[Ar] = 3.89 \times 10^{-5}$ mol cm^{-3}; lower panel: single tube traversal of light from Xe lamp, $T = 1086$ K, $[H_2O_2]_0/[Ar] = 2.640 \times 10^{-3}$ $[Ar] = 3.04 \times 10^{-5}$ mol cm^{-3}).

215 nm, we relied on the absorption coefficient under these conditions. A value of

$$\varepsilon_{215}(H_2O_2) = 84.1\,(\pm 10\%)\,\mathrm{l\,mol^{-1}\,cm^{-1}}$$

from refs. 23 and 24 throughout this work was used as the reference value, all our determinations being made relative to

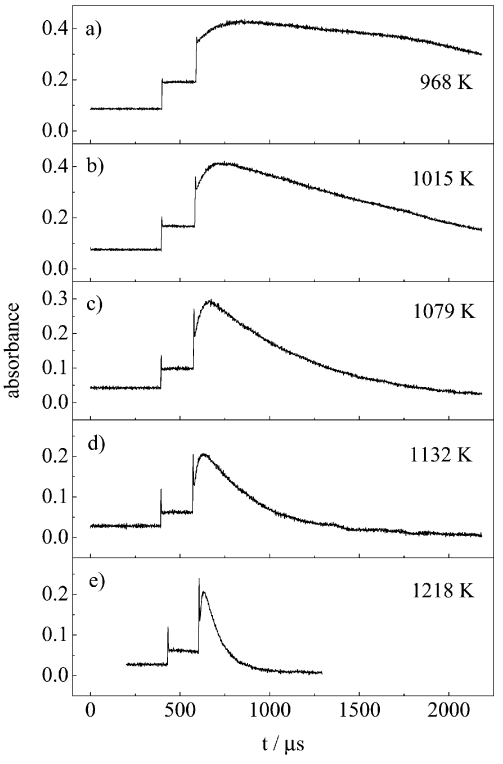

Fig. 2 Absorption signals at 215 nm ($T = 968$ K (a), 1015 (b), 1079 (c), 1132 (d), 1218 K (e); $[H_2O_2]_0/[Ar] = 3.112$ (a), 3.182 (b), 1.954 (c), 1.361 (d), 1.711 (e) $\times 10^{-3}$, $[Ar] \times 10^5$ mol cm^{-3} = 4.57 (a), 3.96 (b), 3.89 (c), 3.82 (d), 3.04 (e)).

this value. As the schlieren signals at the absorption steps of the incident and reflected shocks in Figs. 1 and 2 are well defined, an extrapolation to the time before the onset of reaction could be made reliably. The resulting absorption coefficients of H_2O_2 at 215 and 230 nm are represented by

$$\varepsilon_{215}(H_2O_2)/l\,mol^{-1}\,cm^{-1} = 96.0(\pm 6.7) - (0.019 \pm 0.006)T/K$$

$$\varepsilon_{230}(H_2O_2)/l\,mol^{-1}\,cm^{-1} = 68.4(\pm 5.8) - (0.004 \pm 0.005)T/K$$

for the temperature range 950–1250 K. These results appear consistent with our earlier analysis of the temperature dependence of ε,[4] although a much larger precision is now available.

3.2 Absorption coefficients of HO_2

At the time of the identification of the HO_2 spectrum in 1969,[2] the absorption coefficient of HO_2 had to be determined by an analysis of the kinetics of reactions (1)–(4) in comparison to the recorded superimposed HO_2 and H_2O_2 absorption signals. It was realized already in[4] that room temperature[19] and shock wave[2] absorption coefficients of HO_2 in the gas phase are surprisingly consistent in relation to each other. In the meantime, the temperature dependence of ε_{HO_2} has been characterized more quantitatively,[20] see Fig. 3. For this reason, it appeared preferable not to fit ε_{HO_2} *via* our recorded absorption signals but to use extrapolations of the direct determinations which were made up to 777 K.[20] We, therefore, employed

$$\varepsilon_{215}(HO_2)/l\ mol^{-1}\ cm^{-1} = 1155\ [1 - \exp(-1299\,K/T)]$$

and

$$\varepsilon_{230}(HO_2)/l\ mol^{-1}\ cm^{-1} = 615$$

from ref. 20 which essentially is in agreement with earlier results.[4] The uncertainty of $\varepsilon(HO_2)$ here is estimated to be about 10 percent.

3.2 Dissociation rate constant k_1 of H_2O_2

The rate constant k_1 of the primary dissociation, reaction (1), of H_2O_2 was determined in a variety of ways. It was shown[2] that HO_2 practically does not absorb at 290 nm while H_2O_2 still absorbs at this wavelength. In spite of the fact that the H_2O_2 absorption at 290 nm is only weak, reliable concentration-time profiles of H_2O_2 here can be recorded. A preliminary simulation with literature values of k_1–k_4 shows that the reaction, after a time which is also reflected by the maxima of the superimposed H_2O_2 and HO_2 signals in Fig. 1 and 2, approaches steady state with an apparent decay constant k

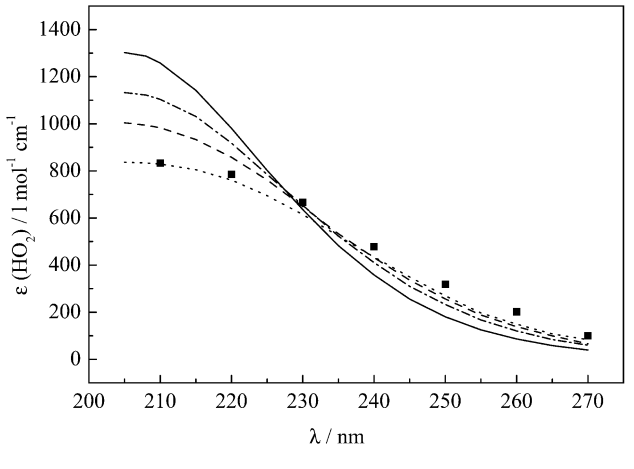

Fig. 3 Decadic absorption coefficients ε of HO_2 (■: shock wave results from ref. 2, see text; —: 298 K, –·–: 577 K, ---: 777 K, ···: 1100 K, experiments and representation from ref. 20).

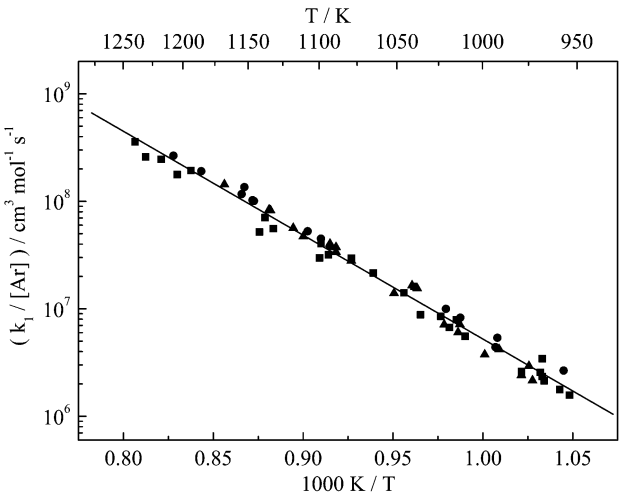

Fig. 4 Pseudo-second order rate constants k_1/[Ar] of the unimolecular dissociation of H_2O_2: experiments with threefold (■) and single (▲) tube traversal of analysis light at 215 nm and single traversal (●) at 230 nm.

of the H_2O_2-absorption signals given by $k = 2k_1$. In addition, measurements at 215 (or 230) nm, after a full interpretation of the superimposed H_2O_2- and HO_2-profiles (see below), lead to k_1. We indeed observed good agreement between the two determinations, although the small absorption signals at 290 nm produced a slightly larger scatter of the results than the measurements at 215 and 230 nm.

An Arrhenius plot of our present results, for a bath gas pressure of 4 bar, is shown in Fig. 4. It can be represented by

$$k_1(4\ bar)/cm^3\,mol^{-1}\,s^{-1} = [Ar]10^{16.02\pm0.14}\exp[-21\,437\,(\pm 343)\,K/T]$$

over the temperature range 950–1250 K.

By comparison of measurements at 4 and 20 bar, our earlier experiments[1] revealed a small deviation of the rate constant k_1 from pseudo-second order behaviour, suggesting, however, that reaction (1) under typical shock wave conditions is close to the limiting low pressure range. In view of the fall-off results recorded for the reverse recombination, reaction (−1),[16–17] we now more carefully investigated the pressure dependence of the pyrolysis. By performing experiments at Ar pressures of 1, 4, and 15 bar, the deviation from second order behaviour of reaction (1) could be documented more clearly. Fig. 5 shows

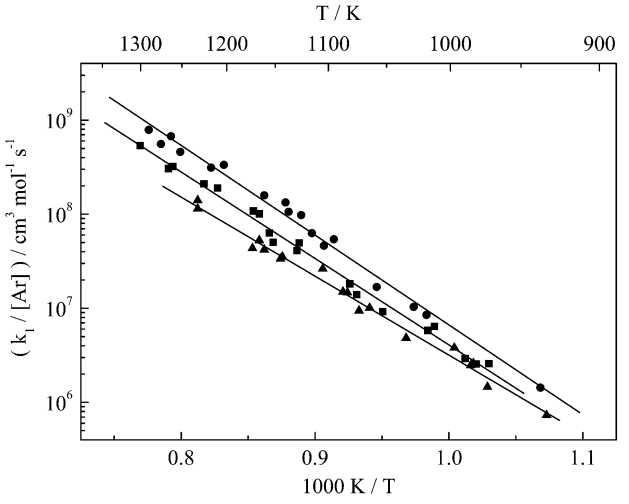

Fig. 5 Pseudo-second order rate constants k_1/[Ar] at 1 bar (●), 4 bar (■), and 15 bar (▲) of Ar.

Table 1 Selected experimental results

(a) Measurements near 4 bar

T/K	$[Ar]/10^{-5}$ mol cm^{-3}	$[H_2O_2]_0/10^{-7}$ mol cm^{-3}	$k_1/[Ar]/10^7$ cm^3 mol^{-1} s^{-1}	$k_3/10^{12}$ cm^3 mol^{-1} s^{-1}	k_4/k_2
954	4.21	1.31	0.16	0.74	5.5
967	3.99	0.59	0.21	0.78	5.5
968	4.52	1.42	0.34	0.78	4
1015	3.96	1.29	0.79	0.94	4
1024	4.28	0.50	0.85	0.83	3
1065	4.16	0.97	2.16	0.97	2.5
1079	3.89	0.76	2.96	0.93	3.25
1099	3.85	1.24	4.04	0.91	4
1132	3.82	0.52	5.58	1.14	3.5
1138	3.24	0.52	7.06	1.05	3.25
1194	3.52	1.09	10.9	0.98	3
1218	3.04	0.52	24.6	1.55	2.5
1240	3.00	0.76	35.8	1.50	3

(b) Measurements near 1 and 15 bar

T/K	$[Ar]/10^{-5}$ mol cm^{-3}	$[H_2O_2]_0/10^{-7}$ mol cm^{-3}	$k_1/[Ar]/10^7$ cm^3 mol^{-1} s^{-1}
1017	0.86	0.99	0.85
1057	0.85	0.90	1.69
1103	0.85	0.88	4.62
1136	0.83	1.05	10.6
1202	0.77	1.31	33.4
1251	0.71	0.91	45.9
1289	0.73	1.04	78.6
972	19.6	1.49	0.15
984	18.2	1.45	0.25
1033	18.0	1.15	0.48
1082	16.7	1.81	1.47
1142	16.2	1.65	3.52
1172	15.3	1.19	4.34
1231	14.4	1.36	11.4

pseudo-second order plots of our results. The pseudo-first order rate constants are represented by

$$k_1(1\,\text{bar})/\text{cm}^3\,\text{mol}^{-1}\,\text{s}^{-1} = 10^{16.36\pm0.24}\exp[-21\,962\,(\pm608)\,\text{K}/T]$$

$$k_1(15\,\text{bar})/\text{cm}^3\,\text{mol}^{-1}\,\text{s}^{-1} = 10^{14.90\pm0.20}\exp[-19\,330\,(\pm504)\,\text{K}/T].$$

Selected experimental results are summarized in Table 1. In comparison to the measurements at lower pressures, one would have expected a higher apparent activation energy for the experiments at higher pressures. Experimental scatter apparently hides this normal behaviour of falloff curves.

3.3 Rate constants k_2–k_4 of secondary reactions

The quality of the earlier absorption-time profiles was such that essentially only the position and the height of the maxima of the superimposed H_2O_2 and HO_2 signals could be exploited for a determination of $\varepsilon(HO_2)$ and of the ratios k_3/k_2 and k_4/k_2 as a function of the ratio $k_2[H_2O_2]_0/k_1[Ar]$.[2] The much improved quality of the present absorption-time profiles allowed us to fit the full absorption-time profiles leading to more reliable rate parameters. In doing this, $\varepsilon(HO_2)$, $[H_2O_2]_0$, and k_1 were fixed as described in sections 3.1–3.3. Careful analysis of the sensitivity of our set of absorption–time profiles showed that our observations, apart from the fixed parameters given above, are sensitive not to the ratios k_3/k_2 and k_4/k_2, but only k_3 and the ratio k_4/k_2. Fig. 6 demonstrates the corresponding sensitivities and the quality of the agreement between experiment and simulation. It may appear from Fig. 6 that k_3 and k_4/k_2 cannot be fitted independently, and that an increase of k_3 could be compensated by the corresponding decrease of the ratio k_4/k_2. However, the fine details of the profiles, maxima and curvatures near to and further away from the maxima of the absorptions, clearly allowed for a distinction between k_3 and k_4/k_2. This distinction was even more supported by experiments with changing initial concentrations $[H_2O_2]_0$. A necessary condition for the optimum fit of k_3 and k_4/k_2, however, was the precise characterization of k_1 in each individual experiment. The sensitivity of the profiles on k_1 is also demonstrated in Fig. 6.

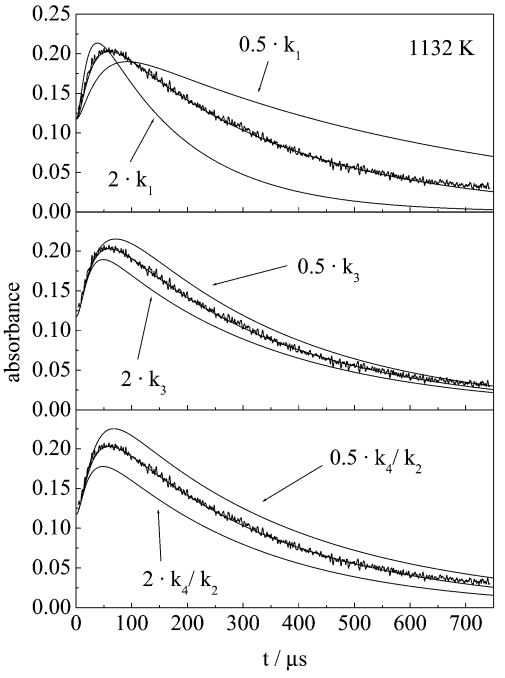

Fig. 6 Sensitivity of recorded absorption profiles on k_1, k_3, and k_4/k_2 at 1132 K, $[Ar] = 3.82 \times 10^{-5}$ mol cm^{-3}, $[H_2O_2]_0/[Ar] = 1.361 \times 10^{-3}$.

The results from the described analysis of the absorption–time profiles are shown in Figs. 7 and 8. They are represented by

$$k_3/\text{cm}^3\,\text{mol}^{-1}\,\text{s}^{-1} = 10^{13.05\pm0.06}\exp[-2653\ (\pm159)\ \text{K}/T]$$

and

$$k_4/k_2 = 2.99\ (\pm0.21) + 6.72\ (\pm0.8) \times 10^{-7}\exp[T/62.4\ (\pm20)\ \text{K}].$$

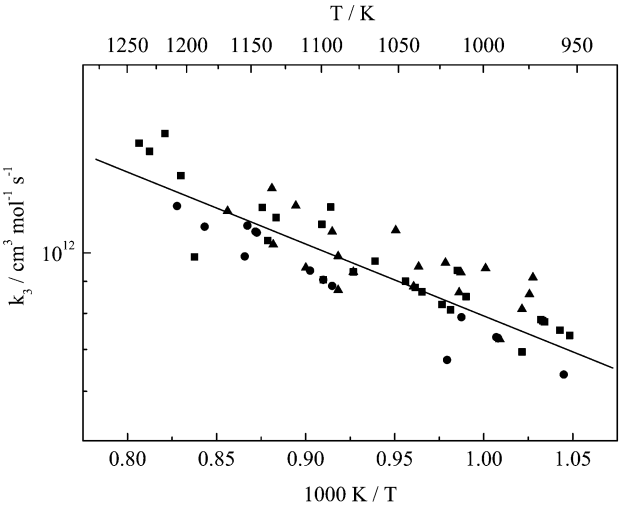

Fig. 7 Rate constants k_3 (symbols as in Fig. 4, full line: expression from section 3.4).

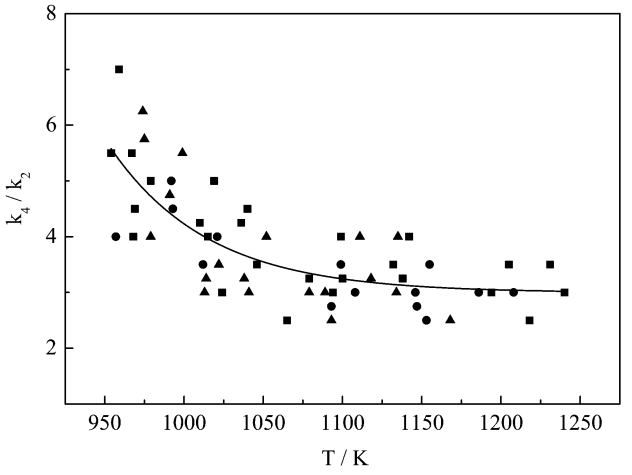

Fig. 8 Rate constant ratio k_4/k_2 (symbols as in Fig. 4, full line: expression from section 3.4.

The scatter of the data in part corresponds to the scatter of the values of $k_1[H_2O_2]_0$ entering the simulation; in part it reflects the remaining fitting uncertainties of the absorption time profiles.

4. Discussion

4.1 Unimolecular dissociation of H_2O_2

The present results for k_1 improve our earlier determinations[2] which were also based on H_2O_2 and HO_2 profiles. There is good agreement between the present results for 4 and 15 bar and the corresponding data from ref. 1 before temperature corrections of the latter were made in ref. 4. The present work, however, indicates that the temperature corrections made in ref. 4 which were based on the assumptions of considerable pre-shock decomposition of H_2O_2 changing the composition of the reaction mixtures, were unjustified. By extending experiments down to 1 bar, the present work provided a larger part of the falloff curves near to the low pressure limit than was accessible before. Fig. 9 demonstrates the pressure dependences together with preliminary constructions of falloff curves, following refs. 25–27 with $F_{cent} \approx 0.5$, see below.

The pyrolysis of H_2O_2 provides one of the rare cases where shock wave experiments overlap with experiments from static or flow reactors. Besides the measurements in refs. 8–11 and 13 at $T < 830$ K, low pressure flow system measurements[12] reached up to 932 K, *i.e.* practically the lowest temperatures of the present work. These experiments led to $k_1 = [N_2]$ 2.3×10^6 cm^3 mol^{-1} s^{-1} at 919 K while the present work, with an only short extrapolation from 950 to 919 K, gave $k_1 = [Ar]$ 9.6×10^5 cm^3 mol^{-1} s^{-1}. Most of the difference of a factor of 2.4 is due to the fact that the bath gas N_2 in ref. 12 contained 10% of H_2O and 5% of H_2O_2 which, because of the ten times larger efficiencies of H_2O and H_2O_2 in comparison to N_2,[13] should increase k_1 by about the same factor of 2.4. In addition, small differences in the efficiencies of N_2 and Ar, small falloff corrections between the experiments from ref. 12 (at 5–7 Torr) and our actual work (at 1 bar), as well as some problems with heterogeneous reactions in ref. 12 may have been present. In view of these various contributions, the agreement between our shock wave results and the flow system data from ref. 12 appears quite satisfactory.

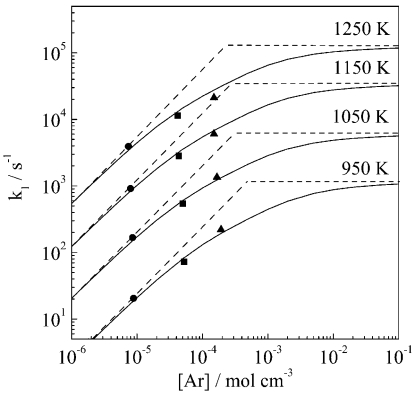

Fig. 9 Falloff curves of k_1 (symbols: experimental points; full lines: calculated curves with $F_c = 0.5$, see text).

The experimental falloff curves of the present work in Fig. 9 are tentatively compared with modelled curves based on the expression[25]

$$k/k_\infty = [x/(1+x)]F(x) \quad (5)$$

with $x = k_0/k_\infty$,

$$F(x) = F_{cent}^{\left[1+(\log x/N)^2\right]^{-1}}, \quad (6)$$

$N = 0.75–1.27 \log F_{cent}$, and the first guess of $F_{cent} \approx 0.5 \pm 0.05$ from ref. 27. k_1 (1 bar) such as given above, was used for k_0. The extrapolation towards k_∞ then gave $k_\infty/s^{-1} \approx 4 \times 10^{11}$ exp(−18 690 K/T), this value, however, being fairly uncertain for the following reasons. First, only the low pressure part of the falloff curves was measured such that the scatter of the data prevents a meaningful extrapolation towards k_∞. Second, the detailed investigations in part II of this work[28] provide a better representation of the falloff curves from statistical unimolecular rate theory than given by the standard procedure in refs. 25,26. Finally, the classical trajectory calculations[28] on the *ab initio* potential of H_2O_2 from ref. 22 provide evidence about highly non-exponential lifetime distributions of excited H_2O_2. It is known[29] that this leads to broader falloff curves than obtained by statistical unimolecular rate theory. For this reason, the present extrapolation towards k_∞ does not give meaningful results. A more detailed interpretation of k_0 and the observed pressure dependences of k_1, therefore, requires extensive theoretical work which will be described in part II.[28]

The present dissociation results should be compared with recombination data using the relationship

$$k_1/k_{-1} = K_c. \quad (7)$$

We employ

$$K_c = 5.87 \times 10^{25} \exp(-24\,660\ \text{K}/T)\ \text{molecule cm}^{-3}$$

between 950 and 1250 K. This value is based on the thermodynamic data from ref. 30 after the value of the dissociation energy of H_2O_2 of $D_0 = 17\,269.4$ cm^{-1} used in ref. 30 has been corrected to the spectroscopic value of $D_0 = 17\,051.8$ ($\pm$3.4) cm^{-1} from ref. 31. The latter change is consistent with the recent revision of the enthalpy of formation of HO[32] in combination with the enthalpy of formation of H_2O_2 from ref. 33 which in turn also appears consistent now. With K_c and our $k_{1,0}$ one obtains $k_{-1,0}$/cm^6 molecule^{-2} s^{-1} = 7.4×10^{-33} [Ar] at 1000 K which appears roughly consistent with the recombination measurements from ref. 17 (after the temperature dependence of the competing reaction HO + HO → H_2O + O in ref. 34 has been refined). On the other hand, the tentative value of $k_{1\infty}(1000\ \text{K})/s^{-1} \approx 3.1 \times 10^3$ gives $k_{-1,\infty}$/cm^3 molecule^{-1} s^{-1} $\approx 2.7 \times 10^{-12}$ which falls about a factor of 10 below extrapolations of the experimental data from ref. 17 and the theoretical predictions from ref. 28. Part II explains this discrepancy and provides a more

quantitative analysis of the high and low pressure limiting rate constants as well as of the falloff curves of this dissociation and recombination reaction.

4.2 Rate constants of secondary reactions

On the basis of the present determinations of k_1, k_3 and k_4/k_2, at first, we have reevaluated the OH-absorption–time profiles which were recorded[7] during the H_2O_2 pyrolysis. These profiles allowed us to fit the value of k_2 sensitively. It turned out that the present changes of rate constants had no influence on k_2 such that the value from ref. 7 for the temperature range of 950–1250 K was reconfirmed. The non-Arrhenius temperature dependence of k_2 from ref. 7 is expressed by

$$k_2/\mathrm{cm^3\,mol^{-1}\,s^{-1}} = 1.7 \times 10^{18}\exp(-14\,800\,\mathrm{K}/T) + 2.0 \times 10^{12}\exp(-215\,\mathrm{K}/T)$$

over the range 240–1600 K.

Fig. 10 compares the present data for k_3 with our earlier results and determinations at lower temperatures.[35–37] The rate constant minimum near 800 K is clearly observed again. While some pressure dependence of k_3 at temperatures below 800 K was detected in refs. 35–37 we have not found such effects under our conditions. Our present results near 1200 K are somewhat lower than the earliest determination[2] which is superseded by the present more complete analysis. The slight disagreement with our data[5] is more irritating. In ref. 5 k_3 was determined in two ways, from HO_2 signals in the pyrolysis of H_2O_2 and after HO_2 formation through the reaction $H + O_2$ following the pyrolysis of CH_3O formed from CH_3OOCH_3. A value of $k_3(1000\ \mathrm{K})/\mathrm{cm^3\,mol^{-1}\,s^{-1}} = 1.3 \times 10^{12}$ was obtained in contrast to the present result of 7.9×10^{11}. Since the present determinations showed much less scatter, they should be more reliable. Nevertheless, apart from the small difference, the values of k_3 appear well established now. The combination of the present and previous low temperature data from refs. 35–37 such as shown in Fig. 10 gives

$$k_3/\mathrm{cm^3\,mol^{-1}\,s^{-1}} = 1.03 \times 10^{14}\exp(-5556\,\mathrm{K}/T) + 1.94 \times 10^{11}\exp(+709\,\mathrm{K}/T)$$

over the range 300–1250 K.

Employing the value of k_2 such as given above, our present experimental result for the ratio k_4/k_2 can be converted into values of k_4. Fig. 11 compares these values with our earlier results from ref. 7 and literature data for higher[38,39] and lower temperatures.[40–42] Most importantly, the deep and unusually narrow rate constant minimum, such as derived

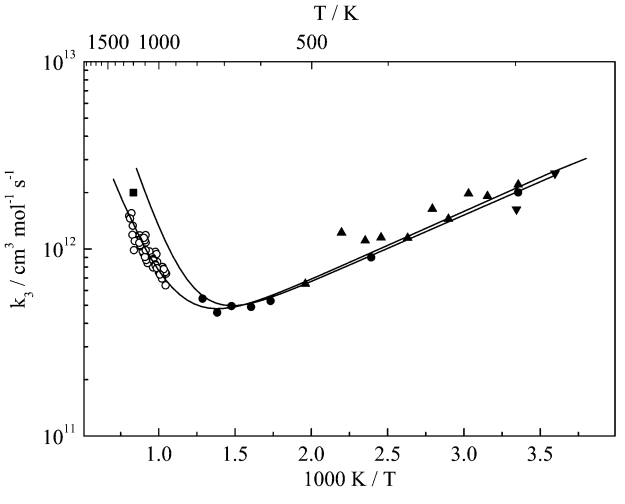

Fig. 10 Rate constants k_3 (■: ref. 2, ▲: ref. 35, ▼: ref. 36, ●: ref. 37, ○ and lower line: this work, upper line: ref. 5).

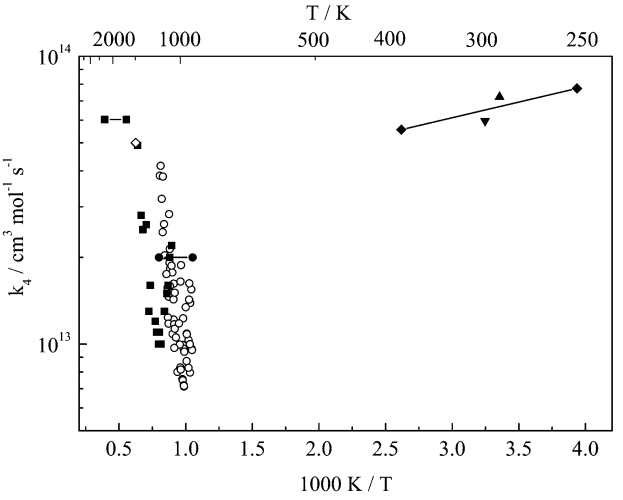

Fig. 11 Rate constants k_4 (▼: ref. 40, ▲: ref. 41, –◆–: ref. 42, ◆: ref. 38, –■–: ref. 39, –●–: ref. 6, ■: ref. 7, ○: this work).

first from HO absorption-time profiles in the pyrolysis of H_2O_2,[7] was reconfirmed. In contrast to a minimum near to 1200 K,[7] we now observed the minimum nearer to 1000 K. The determination of k_4 is sensitive to the concentration of the reactants. For this reason, the more direct and accurate determination of the initial concentration of H_2O_2 probably makes the present results more reliable than our earlier data. However, the problems of separating k_3 and k_4/k_2 such as described above leave some uncertainty. Therefore, we only note the relatively good agreement between the two determinations of k_4 which employed two different methods (HO_2- and HO-profiles) and which both show the deep and narrow rate constant minimum. The combination of k_2 and the present ratio k_4/k_2, see above, leads to values of

$$k_4/\mathrm{cm^3\,mol^{-1}\,s^{-1}} = 1.0 \times 10^{13} + 5.8 \times 10^{13}\exp[-2000\,\mathrm{K}/T]$$

over the range 950–1250 K. It is difficult to combine these results with low temperature data into a common expression. This has to wait until new data are available for the intermediate range between 400 and 900 K.

5. Conclusions

The present work provides experimental evidence for an unexpected early onset of deviations from the limiting low pressure behaviour of the unimolecular dissociation of H_2O_2. As a consequence, conventional falloff extrapolations towards the high pressure limit lead to values which are markedly below calculational results, employing the *ab initio* potential of H_2O_2 such as described in part II of this series.[28] These observations are of interest in relation to classical trajectory calculations of dissociative lifetimes of H_2O_2 which led to strongly non-exponential lifetime distributions.[28] A theoretical analysis of the temperature and pressure dependences of the dissociation of H_2O_2 and the reverse recombination of HO radicals, which also accounts for this effect, is left for part II of this series. The present shock wave results were shown to be quantitatively consistent with flow system results from ref. 12 which were obtained (almost) exactly up to the lowest temperatures of the present study.

The much improved accuracy of the present work in comparison to earlier studies allowed us to characterize dissociation rates, high temperature absorption spectra of H_2O_2 and of HO_2, and rate constants of the reactions $HO + H_2O_2 \rightarrow HO_2 + H_2O$, $HO_2 + HO_2 \rightarrow H_2O_2 + O_2$, and $HO + HO_2 \rightarrow H_2O + O_2$ with larger reliability than this was possible before.

The highly non-Arrhenius temperature dependence of the latter three reactions was confirmed. The present determinations of the rate constants of the latter two reactions differed slightly from our earlier results. However, the previously observed rate constant minima were confirmed. In particular, the very deep minimum of the last reaction, which earlier was derived from HO absorption-time profiles, now was also determined from HO_2 absorption-time profiles. The results on these three reactions strongly suggest pathways involving bound intermediate complexes. They call for *ab initio* calculations of the potentials combined with classical trajectory calculations of the dynamics on these potentials.

Acknowledgements

Financial support of this work by the Deutsche Forschungsgemeinschaft (SFB 357 "Molekulare Mechanismen unimolekularer Reaktionen") is gratefully acknowledged.

References

1 E. Meyer, H. A. Olschewski, J. Troe and H. Gg. Wagner, *Proc. Combust. Inst.*, 1968, **12**, 345.
2 J. Troe, *Ber. Bunsen-Ges. Phys. Chem.*, 1969, **73**, 946.
3 H. Kijewski and J. Troe, *Int. J. Chem. Kinet.*, 1971, **3**, 223.
4 H. Kijewski and J. Troe, *Helv. Chim. Acta*, 1972, **55**, 205.
5 H. Hippler, J. Troe and J. Willner, *J. Chem. Phys.*, 1990, **93**, 1755.
6 H. Hippler and J. Troe, *Chem. Phys. Lett.*, 1992, **192**, 333.
7 H. Hippler, H. Neunaber and J. Troe, *J. Chem. Phys.*, 1995, **103**, 3510.
8 C. K. McLane, *J. Chem. Phys.*, 1949, **17**, 379.
9 C. N. Satterfield and T. W. Stein, *J. Phys. Chem.*, 1957, **61**, 537.
10 P. A. Giguère and I. D. Liu, *Can. J. Chem.*, 1957, **35**, 283.
11 W. Forst, *Can. J. Chem.*, 1958, **36**, 1308.
12 D. E. Hoare, J. B. Prothero and A. D. Walsh, *Trans. Faraday Soc.*, 1959, **55**, 548.
13 R. R. Baldwin and D. Brattan, *Proc. Combust. Inst.*, 1960, **8**, 110.
14 D. W. Trainor and C. W. von Rosenberg, *J. Chem. Phys.*, 1974, **61**, 1010.
15 R. Zellner, F. Ewig, R. Paschke and G. Wagner, *J. Phys. Chem.*, 1988, **92**, 4184.
16 R. Forster, M. Frost, D. Fulle, H. F. Hamann, H. Hippler, A. Schlepegrell and J. Troe, *J. Chem. Phys.*, 1995, **103**, 2949.
17 D. Fulle, H. F. Hamann, H. Hippler and J. Troe, *J. Chem. Phys.*, 1996, **105**, 1001.
18 J. Troe, *J. Chem. Soc., Faraday Trans.*, 1994, **90**, 2303.
19 T. T. Paukert and H. S. Johnston, *J. Chem. Phys.*, 1972, **56**, 4426.
20 (*a*) P. D. Lightfoot and A. A. Jemi-Alade, *J. Photochem. Photobiol., A: Chem.*, 1991, **59**, 1; (*b*) J. N. Crowley, F. G. Simon, J. P. Burrows, G. K. Moortgat, M. E. Jenkin and R. A. Cox, *J. Photochem. Photobiol., A: Chem.*, 1991, **60**, 1.
21 (*a*) L. B. Harding, *J. Phys. Chem.*, 1989, **93**, 8004; (*b*) 1991, **95**, 8653
22 B. Kuhn, T. R. Rizzo, D. Luckhaus, M. Quack and M. A. Suhm, *J. Chem. Phys.*, 1999, **111**, 2565.
23 L. B. Ghanshyam and A. R. Ravishankara, *J. Geophys. Res.*, 1989, **94**, 3487.
24 E.-P. Röth, R. Ruhnke, G. Moortgat, R. Meller, and W. Schneider, *UV/VIS-Absorption Cross Sections and Quantum Yields for Use in Photochemistry and Atmospheric Modeling*, Forschungszentrum Jülich, Germany 1997.
25 J. Troe, *Ber. Bunsen-Ges. Phys. Chem.*, 1983, **87**, 161.
26 R. G. Gilbert, K. Luther and J. Troe, *Ber. Bunsen-Ges. Phys. Chem.*, 1983, **87**, 169.
27 L. Brouwer, C. Cobos, J. Troe, H.-R. Dübal and F. F. Crim, *J. Chem. Phys.*, 1987, **86**, 6171.
28 J. Troe and V. G. Ushakov, Part II of this series, in preparation.
29 R. C. Baetzold and D. J. Wilson, *J. Phys. Chem.*, 1964, **68**, 3141.
30 *NIST-JANAF Thermochemical Tables*, 4th edn., (1998; J. Phys. Chem. Ref. Data Monograph No 9).
31 X. Luo, P. R. Fleming and T. R. Rizzo, *J. Chem. Phys.*, 1992, **96**, 5659.
32 B. Ruscic, A. F. Wagner, L. B. Harding, R. L. Asher, D. Feller, D. A. Dixon, K. A. Peterson, Y. Song, X. Qian, C.-Y. Ng, J. Lin, W. Chen and D. W. Schwenke, *J. Phys. Chem. A*, 2002, **106**, 2727.
33 (*a*) P. A. Giguère and I. D. Lin, *J. Am. Chem. Soc.*, 1955, **77**, 6477; (*b*) P. A. Giguère, B. G. Morisette, A. W. Olmos and O. Knop, *Can. J. Chem.*, 1955, **33**, 804.
34 Y. Bedjanian, G. Le Bras and G. Poulet, *J. Phys. Chem. A*, 1999, **103**, 7017.
35 R. Patrick and M. Pilling, *Chem. Phys. Lett.*, 1982, **91**, 343.
36 B. Y. Andersson, R. A. Cox and M. E. Jenkins, *Int. J. Chem. Kinet.*, 1988, **20**, 283.
37 P. D. Lightfoot, B. Veyret and R. Lesclaux, *Chem. Phys. Lett.*, 1988, **150**, 120.
38 J. Peeters and G. Mahnen, *Proc. Combust. Inst.*, 1972, **14**, 133.
39 J. M. Goodings and A. N. Hayhurst, *J. Chem. Soc., Faraday Trans. 2*, 1988, **84**, 745.
40 R.-R. Lii, R. A. Corse, M. C. Sauer and S. Gordon, *J. Phys. Chem.*, 1980, **84**, 819.
41 W. B. DeMore, *J. Phys. Chem.*, 1982, **86**, 121.
42 L. F. Keyser, *J. Phys. Chem.*, 1988, **92**, 1193.